

# Infrared Spectroscopic Study on the Surface Properties of $\gamma$ -Gallium Oxide as Compared to Those of $\gamma$ -Alumina

A. Vimont,<sup>\*,†</sup> J. C. Lavalley,<sup>†</sup> A. Sahibed-Dine,<sup>‡</sup> C. Otero Areán,<sup>§</sup> M. Rodríguez Delgado,<sup>§</sup> and M. Daturi<sup>†</sup>

Laboratoire Catalyse et Spectrochimie, UMR 6506, CNRS-ENSICAEN, University of Caen, 6 Bd Maréchal Juin, F-14050 Caen Cedex, France, Faculté des Sciences, Université Chouaib Doukkali, B. P. 20 El Jadida, Morocco, and Departamento de Química, Universidad de las Islas Baleares, 07122 Palma de Mallorca, Spain

Received: January 7, 2005; In Final Form: March 14, 2005

By hydrolysis of an ethanolic gallium nitrate solution,  $\gamma$ -Ga<sub>2</sub>O<sub>3</sub> was prepared as a single-phase polymorph having a specific surface area of 160 m<sup>2</sup> g<sup>-1</sup>. Surface acidity and basicity of this material was studied by IR spectroscopy, using pyridine, 2,6-dimethylpyridine, acetonitrile, and carbon dioxide as spectroscopic probe molecules. For comparison, a  $\gamma$ -Al<sub>2</sub>O<sub>3</sub> sample having a surface area of 290 m<sup>2</sup> g<sup>-1</sup> was also studied. On partially hydroxylated  $\gamma$ -Ga<sub>2</sub>O<sub>3</sub>, the main O–H stretching bands were found at 3693 (sharp) and at 3660–3630 cm<sup>-1</sup> (broad), and the material proved (by adsorbed dimethylpyridine) to have a weak Brønsted acidity. Surface Lewis acidity of  $\gamma$ -Ga<sub>2</sub>O<sub>3</sub> was revealed (mainly) by adsorbed pyridine, which gave the characteristic IR absorption bands of Lewis-type adducts at 1612, 1579, 1488, and 1449 cm<sup>-1</sup> (values noted under an equilibrium pressure of 1 Torr at room temperature); the corresponding Lewis acid centers (coordinatively unsaturated Ga<sup>3+</sup> ions) were found to be weaker, although more abundant, than those present on the surface of  $\gamma$ -Al<sub>2</sub>O<sub>3</sub> (unsaturated Al<sup>3+</sup> ions). Another significant difference between  $\gamma$ -Ga<sub>2</sub>O<sub>3</sub> and  $\gamma$ -Al<sub>2</sub>O<sub>3</sub> is the smaller thermal stability of pyridine and 2,6-dimethylpyridine Lewis adducts formed on the gallium oxide. The surface basicity of  $\gamma$ -Ga<sub>2</sub>O<sub>3</sub> was studied by using carbon dioxide and deuterated acetonitrile as IR probe molecules. Adsorbed CO<sub>2</sub> gave carbonate and hydrogen–carbonate surface species similar to those formed by  $\gamma$ -Al<sub>2</sub>O<sub>3</sub>. Adsorbed acetonitrile gave rise to acetamide species, which revealed the basic character of surface O<sup>2-</sup> ions. These acetamide species were found to be more abundant on  $\gamma$ -Ga<sub>2</sub>O<sub>3</sub> than on  $\gamma$ -Al<sub>2</sub>O<sub>3</sub>.

## 1. Introduction

Gallium(III) oxide, also known as gallia, can crystallize forming the polymorphs  $\alpha$ ,  $\beta$ ,  $\gamma$ ,  $\delta$ , and  $\epsilon$ . Among these five modifications,  $\beta$ -Ga<sub>2</sub>O<sub>3</sub> is the only thermodynamically stable polymorph; it has a monoclinic structure<sup>1</sup> where Ga<sup>3+</sup> ions occupy both distorted tetrahedral and distorted octahedral sites. The  $\alpha$ -Ga<sub>2</sub>O<sub>3</sub> polymorph has the corundum-type structure, while the  $\delta$  form has the C rare earth oxide structure, which becomes slightly modified in the  $\epsilon$  form<sup>2</sup>. The cubic  $\gamma$ -Ga<sub>2</sub>O<sub>3</sub> polymorph has a (defective) spinel-type structure, similar to that of  $\gamma$ -Al<sub>2</sub>O<sub>3</sub>. In this structure, Ga<sup>3+</sup> ions in  $\gamma$ -Ga<sub>2</sub>O<sub>3</sub> and Al<sup>3+</sup> ions in  $\gamma$ -Al<sub>2</sub>O<sub>3</sub> occupy 21 1/3 of the available 24 cation sites per unit cell, leaving 2 2/3 of these sites vacant. However, in contrast to  $\gamma$ -alumina (which has been extensively studied), few reports on the surface chemistry of  $\gamma$ -gallia can be found in the literature.<sup>1–4</sup> And yet, detailed understanding of the surface properties (acidity and basicity) of  $\gamma$ -Ga<sub>2</sub>O<sub>3</sub> is relevant to catalytic applications, since gallium-containing metal oxides and zeolites can act as efficient catalysts in several industrial processes, among them hydrocarbon dehydrogenation and cyclization,<sup>5–9</sup> methane activation,<sup>10,11</sup> methanol to hydrocarbon conversion,<sup>12</sup> and Friedel–Crafts benzylation and acylation reactions.<sup>13</sup> Also, gallia–alumina

mixed oxides have recently been proposed as convenient catalysts for the abatement of nitrogen oxides.<sup>14–16</sup>

Previous IR spectroscopic<sup>2–4</sup> and microcalorimetric<sup>3</sup> studies on the adsorption of CO on  $\gamma$ -Ga<sub>2</sub>O<sub>3</sub> have shown that this gallia polymorph displays some surface Lewis acidity. The corresponding Lewis acid centers were assigned<sup>2–4</sup> to coordinatively unsaturated Ga<sup>3+</sup> ions located both at regular surfaces of the metal oxide particles and on defective surface sites. However, to a large extent, details are not known. The present work was undertaken with a view to (i) extend the previous studies by using pyridine, 2,6-dimethylpyridine, and acetonitrile as IR probe molecules, for a more complete characterization of surface Lewis acidity, (ii) characterize Brønsted acidity of partially hydroxylated  $\gamma$ -Ga<sub>2</sub>O<sub>3</sub>, and (iii) study surface basicity by means of IR spectroscopy of adsorbed carbon dioxide and acetonitrile. Finally, to gain more insight (and also to facilitate analysis of new data), the results of IR spectroscopic studies on  $\gamma$ -Ga<sub>2</sub>O<sub>3</sub> are compared with those obtained for a  $\gamma$ -Al<sub>2</sub>O<sub>3</sub> sample, prepared and treated under similar conditions as those used for  $\gamma$ -Ga<sub>2</sub>O<sub>3</sub>.

## 2. Experimental Section

The gallia polymorph  $\gamma$ -Ga<sub>2</sub>O<sub>3</sub> was prepared by hydrolysis of an ethanolic gallium nitrate solution with aqueous ammonia diluted in ethanol. The resulting gel was filtered, thoroughly washed with ethanol, and vacuum-dried in a desiccator. The xerogel thus obtained was calcined at 573 K for 1 h to render the phase-pure  $\gamma$ -Ga<sub>2</sub>O<sub>3</sub> polymorph, checked by powder X-ray

\* Author to whom correspondence should be addressed. Phone: +33-231452814. Fax: +33-231452822. E-mail: alexandre.vimont@ensicaen.fr.

<sup>†</sup> Laboratoire Catalyse et Spectrochimie, UMR 6506, CNRS-ENSICAEN, University of Caen.

<sup>‡</sup> Faculté des Sciences, Université Chouaib Doukkali.

<sup>§</sup> Departamento de Química, Universidad de las Islas Baleares.

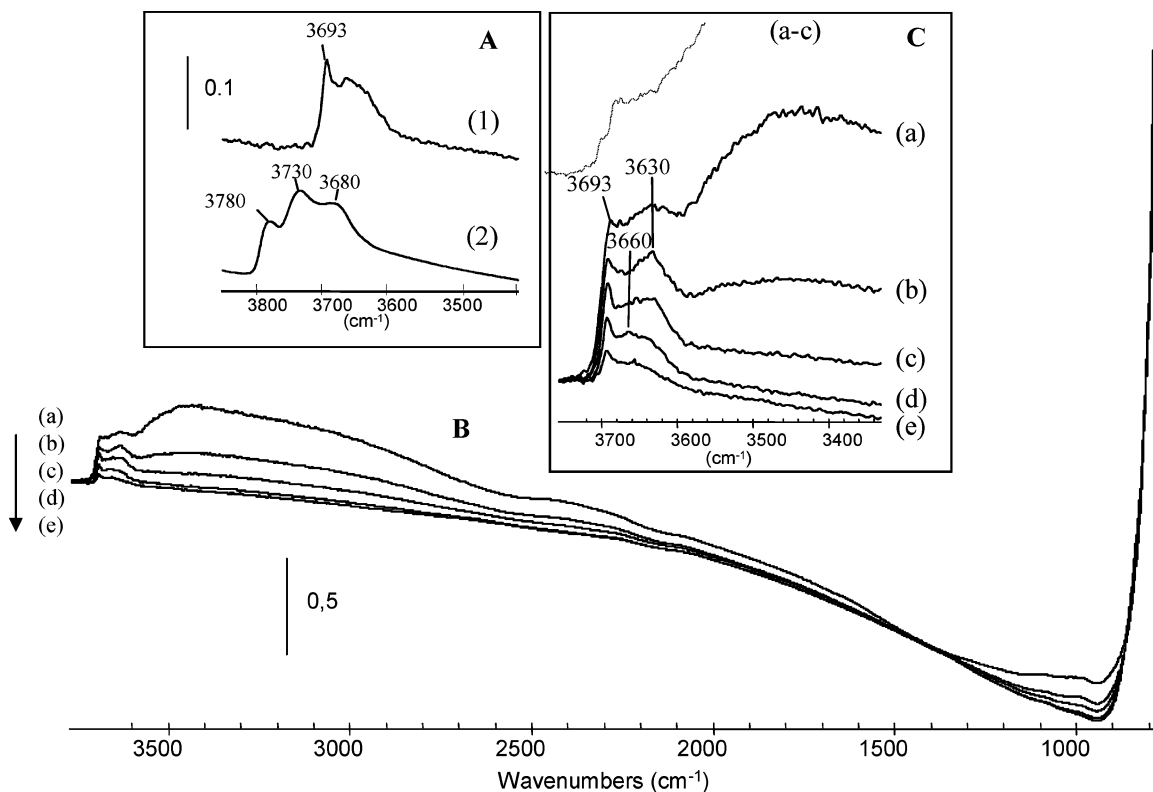


**Figure 1.** IR spectra of  $\gamma$ -Ga<sub>2</sub>O<sub>3</sub> and  $\gamma$ -Al<sub>2</sub>O<sub>3</sub> samples pretreated at 673 K under 100 Torr of O<sub>2</sub> and outgassed at the same temperature for 1 h (spectra A-1 and A-2, respectively).  $\gamma$ -Ga<sub>2</sub>O<sub>3</sub> has then been rehydrated under 10 Torr of water vapor at 373 K and outgassed at an increasing temperature. The corresponding spectra are reported in part B. Spectrum a: After outgassing for 30 min under a vacuum at 373 K. Spectra b–e: After outgassing for 30 min under a vacuum at 473, 573, 673, and 773 K, respectively. Part C shows an enlargement of the same spectra in the 3800–3300 cm<sup>-1</sup> frequency range.

diffraction. Further details were given elsewhere.<sup>2</sup> The  $\gamma$ -Al<sub>2</sub>O<sub>3</sub> polymorph was prepared by calcining at 773 K an alumina gel obtained by adding ammonia to an ethanolic solution of aluminum nitrate and checked by X-ray diffraction. Nitrogen sorption at 77 K showed the above materials to be basically mesoporous. Specific Brunauer–Emmett–Teller (BET) surface areas were 160 and 290 m<sup>2</sup> g<sup>-1</sup> for  $\gamma$ -Ga<sub>2</sub>O<sub>3</sub> and  $\gamma$ -Al<sub>2</sub>O<sub>3</sub>, respectively.

The surface chemistry (acidity and basicity) of the above materials was studied by IR spectroscopy, using adsorbed pyridine, 2,6-dimethylpyridine (DMP), CO<sub>2</sub>, and CD<sub>3</sub>CN as spectroscopic probe molecules. Transmission IR spectra were recorded, at 4 cm<sup>-1</sup> resolution, on a Nicolet Nexus spectrometer equipped with an extended KBr beam splitting device and a mercury cadmium telluride cryodetector. Thin self-supported wafers (2 cm<sup>2</sup>, 8–15 mg) of the metal oxide samples were prepared and thermally activated at 673 K under 100 Torr of O<sub>2</sub> and subsequently outgassed at the same temperature for 1 h under a dynamic vacuum (residual pressure < 10<sup>-6</sup> Torr) inside an IR cell connected to a vacuum line. For IR spectroscopy, accurately known amounts of the probe molecules were dosed into the cell by using a calibrated volume and a pressure gauge (0–100 Torr range). CD<sub>3</sub>CN, pyridine, and DMP (Aldrich, 99+ % grade) were dried on molecular sieves prior to their use. The isotopic purity of CD<sub>3</sub>CN was 99.95%. The exchange H/D procedure to obtain deuterated Gallia was performed on the sample activated at 673 K; adsorption–desorption experiments using D<sub>2</sub>O (1 Torr at equilibrium pressure into the cell at room temperature) were performed four times to achieve a complete H/D exchange of the surface. The sample was then activated under vacuum.

### 3. Results

**3.1. Hydroxy Groups.** Figure 1A shows the IR spectrum in the OH stretching region of  $\gamma$ -Ga<sub>2</sub>O<sub>3</sub> after treatment at 673 K under 100 Torr of O<sub>2</sub> and subsequent outgassing at the same temperature for 1 h. A well-defined band is seen at 3693 cm<sup>-1</sup>; its full width at half-maximum is about 15 cm<sup>-1</sup>. A second, much broader band is observed in the 3700–3580 cm<sup>-1</sup> range. Such a broad band should be due to a group of heterogeneous hydroxyls or to hydroxy groups mutually perturbed by weak hydrogen-bonding interactions.

In the  $\nu$ (OH) range, the spectrum of  $\gamma$ -alumina (Figure 1A, spectrum 2), activated in the same way as above, presents three main  $\nu$ (OH) bands at 3780, 3730, and 3680 cm<sup>-1</sup>, as also reported elsewhere.<sup>17,18</sup> The highest frequency  $\nu$ (OH) band is much broader than that of  $\gamma$ -gallia.

It is well-known that the hydroxylation degree of metal oxide surfaces depends on the pretreatment temperature of the sample, which can strongly modify the nature and surface density of hydroxy groups.<sup>18–21</sup> For a further study of the different OH groups of  $\gamma$ -Ga<sub>2</sub>O<sub>3</sub>, we have rehydroxylated a  $\gamma$ -Ga<sub>2</sub>O<sub>3</sub> sample previously activated at 773 K. To this end, the sample was exposed to water vapor at 373 K, followed by outgassing at an increasing temperature. Corresponding spectra are shown in Figures 1B and 1C. After outgassing at 373 K (spectrum a),  $\nu$ (OH) bands appear in a broad wavenumber range, from 3700 to about 2000 cm<sup>-1</sup>. These  $\nu$ (OH) bands correspond to the metal oxide hydroxy groups, since no band due to molecular water is seen at about 1600–1640 cm<sup>-1</sup> ( $\delta$ (H<sub>2</sub>O) mode). Below 3500 cm<sup>-1</sup>, the  $\nu$ (OH) bands are very broad, and they are similar to those reported for strongly hydroxylated silica and alumina.<sup>20,22</sup> This broadness is due to hydrogen-bonding interactions between

vicinal OH groups that downward shift and broaden the  $\nu(\text{OH})$  bands. Although the  $\gamma$ -gallia surface can be considered as being fully hydroxylated, it is worthwhile to note that the  $3693\text{ cm}^{-1}$  band can be clearly seen, superimposed with a broader one at about  $3630\text{ cm}^{-1}$ . After outgassing at 473 and 573 K, the  $3693\text{ cm}^{-1}$  band becomes gradually better resolved. The subtracted spectra, a minus c in Figure 1C, do not show any noticeable negative peak at this wavenumber value. This fact indicates that the evolution of the  $\nu(\text{OH})$  band at  $3693\text{ cm}^{-1}$ , from a shoulder in spectrum a to a sharp band in spectrum c, is mainly due to the decrease of the broad absorption band at the lower wavenumber when the temperature is raised.

The series of thermal treatments under vacuum from 373 to 573 K (spectra a to c) leads to disappearance of the broad  $\nu(\text{OH})$  band below  $3600\text{ cm}^{-1}$ . Simultaneously, the band at  $3630\text{ cm}^{-1}$  becomes sharper after outgassing at 473 K, and its intensity decreases when outgassing at 573 K. All these features strongly suggest that the  $3693\text{ cm}^{-1}$  hydroxy groups, clearly seen on the fully hydroxylated surface, are not involved in the dehydroxylation process occurring up to 573 K. Outgassing at a higher temperature (Figure 1C, spectra d and e) results in a decreasing intensity of all the persisting  $\nu(\text{OH})$  bands. It is worthwhile noticing that the sharp band at  $3693\text{ cm}^{-1}$  decreases more slowly than the others whereas a new band at  $3660\text{ cm}^{-1}$  seems to develop at the expense of the original low-frequency band at  $3630\text{ cm}^{-1}$ .

**3.2. IR Spectra of Adsorbed Pyridine and DMP.** Surface acidity of the  $\gamma\text{-Ga}_2\text{O}_3$  sample was studied mainly by IR spectroscopy of adsorbed pyridine (Py) and 2,6-dimethylpyridine, and results were compared to those obtained for  $\gamma\text{-Al}_2\text{O}_3$ . Interaction of Py and DMP via the nitrogen lone-pair electrons, with aprotic (Lewis) and protonic (Brønsted) acid sites can be detected by monitoring the ring vibration modes 8a, 8b, 19a, and 19b, named following the nomenclature introduced by Wilson.<sup>23</sup> These modes, which appear at 1598 (8a), 1581 (8b), 1483 (19a), and 1437 (19b)  $\text{cm}^{-1}$  in the IR spectrum of liquid Py and at 1593 (8a), 1580 (8b), 1469 (19a), and 1452 (19b)  $\text{cm}^{-1}$  in the spectrum of liquid DMP, undergo upward frequency shifts upon coordination of the probe molecule to either type of acid sites. Brønsted acidity can be tested by formation of pyridinium species, characterized by bands at about 1640 and  $1545\text{ cm}^{-1}$ , and  $\text{DMPH}^+$  species, characterized by two bands appearing at about 1650 and  $1630\text{ cm}^{-1}$ .

Figure 2A shows the IR spectra of Py adsorbed (at the equilibrium pressure of 1 Torr) on  $\gamma\text{-Ga}_2\text{O}_3$  previously outgassed at 773 K. Characteristic IR absorption bands are seen at 1598, 1483, 1438, 1612, 1579, 1488, and  $1449\text{ cm}^{-1}$  (spectrum 1). The first three of these bands characterize hydrogen-bonded and physisorbed species. Accordingly, they disappear upon desorption at room temperature (Figure 2A, spectrum 2). The remaining bands, which persist upon outgassing at room temperature, identify Lewis-type adducts of adsorbed Py. Two points should be noted. First, the bands of the Lewis-type adducts shift slightly upon partial desorption, due to initial overlap with bands of hydrogen-bonded species. Second, the full width at half-maximum of the bands from the Lewis-type adducts are rather large; the effect is most clearly seen in the  $\nu_{8a}$  band at  $1612\text{ cm}^{-1}$ , which has a full width at half-maximum of about  $19\text{ cm}^{-1}$ .

Lewis-type acidity of the  $\gamma\text{-Ga}_2\text{O}_3$  sample is assigned, in agreement with previous reports,<sup>2,4,24</sup> to coordinatively unsaturated (cus)  $\text{Ga}^{3+}$  ions located on the  $\gamma\text{-Ga}_2\text{O}_3$  surface. No bands were observed at 1640 or  $1545\text{ cm}^{-1}$  in the spectra of adsorbed pyridine, thus showing that the material under study has no Brønsted acid sites strong enough to protonate the adsorbed

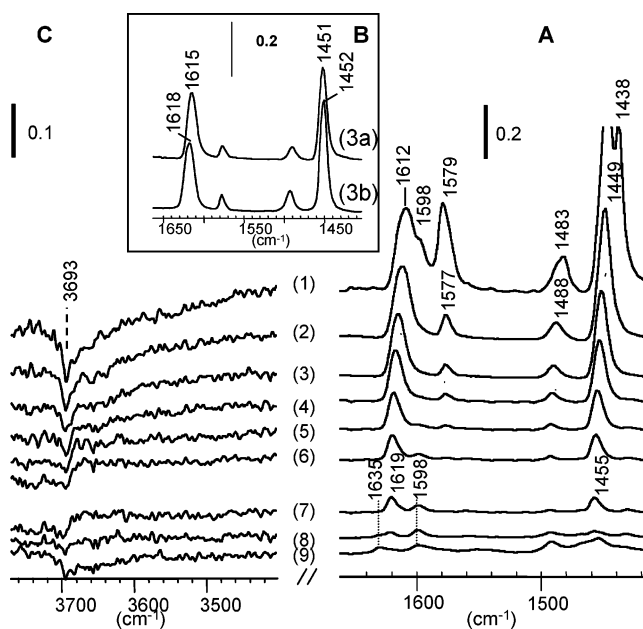


**Figure 2.** (A and C) IR difference spectra (blank subtracted) of pyridine adsorbed on  $\gamma\text{-Ga}_2\text{O}_3$ . Initial equilibrium pressure of 1 Torr (1) followed by outgassing for 30 min at room temperature (2) and then at 373, 423, 473, 523, 573, 673, and 773 K (spectra 3–9, respectively). Inset B: Spectra of adsorbed pyridine on  $\gamma\text{-Ga}_2\text{O}_3$  (3a) and  $\gamma\text{-Al}_2\text{O}_3$  (3b) after pyridine outgassing during 30 min at 373 K.

molecule. When the desorption temperature is increased, the  $\nu_{8a}$  and  $\nu_{19b}$  bands shift from 1612 and  $1449\text{ cm}^{-1}$  to 1619 and  $1455\text{ cm}^{-1}$ , respectively, whereas their intensity strongly decreases. These shifts could be ascribed either to a heterogeneity of the Lewis acid sites, to electronic effects induced by pyridine adsorption, less and less important when pyridine is desorbed, or to both effects.<sup>25</sup> Outgassing at temperatures over 473 K gives rise to new bands at 1635, 1598, and about  $1450\text{ cm}^{-1}$ , which grow as the temperature increases (Figure 2A, spectra 5–9), showing a chemical transformation of pyridine.

In the  $1700\text{--}1400\text{ cm}^{-1}$  range, the IR spectra of pyridine chemisorbed on  $\gamma\text{-Ga}_2\text{O}_3$  and  $\gamma\text{-Al}_2\text{O}_3$  are very similar (Figure 2B, spectra 3a and 3b). The main difference is that on alumina the  $\nu_{8a}$  and  $\nu_{19b}$  vibration bands appear at slightly higher wavenumbers than on gallia. For instance, after outgassing at 373 K, these bands are centered at 1618 and  $1452\text{ cm}^{-1}$  in the case of alumina and at 1615 and  $1451\text{ cm}^{-1}$  in the case of gallia. It is relevant to add that no pyridine decomposition or chemical transformation was detected on alumina, not even after outgassing at 673 K (spectra not shown).

Figure 2C shows the  $\nu(\text{OH})$  region of the  $\gamma$ -gallia sample having adsorbed Py. The evolution of the negative band seen at  $3693\text{ cm}^{-1}$  shows the progressive perturbation of the sharp OH vibration mode (Figure 1A) upon adsorption of pyridine. Note that all spectra have been plotted after subtracting the  $\gamma\text{-Ga}_2\text{O}_3$  blank spectrum. In the case of alumina (spectra not shown), adsorbed pyridine was also found to perturb the  $\nu(\text{OH})$  bands and to a larger extent that at the higher wavenumber ( $3790\text{ cm}^{-1}$ ), as in the case of gallia.

Figure 3 depicts IR spectra of DMP adsorbed at room temperature on  $\gamma\text{-Ga}_2\text{O}_3$ , previously activated at 673 K, and then outgassed at an increasing temperature (spectra 1–7). The three main bands at 1613, 1580, and  $1465\text{ cm}^{-1}$ , which persist after outgassing at room temperature, characterize DMP adducts with Lewis acid sites.<sup>26,27</sup> The very weak band at  $1649\text{ cm}^{-1}$  (Figure 3, spectra 1–4) characterizes protonated DMP species, hence testifying to the presence of a small number of Brønsted



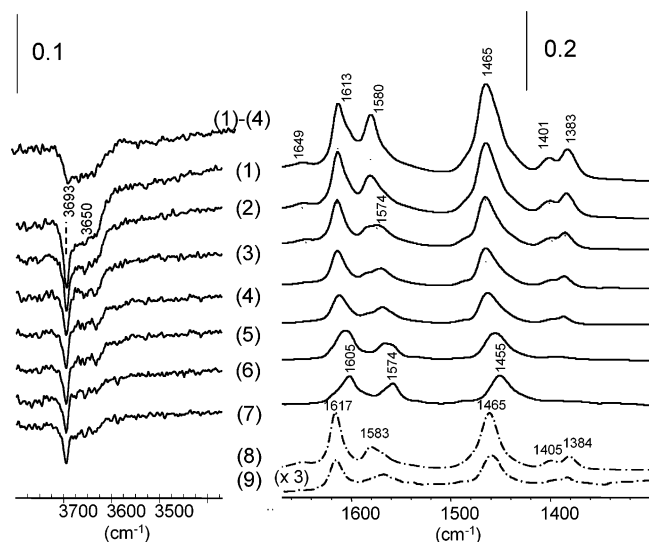


**Figure 3.** IR difference spectra (blank subtracted) of 2,6-dimethylpyridine adsorbed on  $\gamma$ -Ga<sub>2</sub>O<sub>3</sub>. Initial equilibrium pressure of 1 Torr (1) followed by outgassing for 30 min at 323, 373, 423, 473, 573, and 673 K (spectra 2–7, respectively). Dotted lines: Spectra of adsorbed DMP on  $\gamma$ -Al<sub>2</sub>O<sub>3</sub> after outgassing for 30 min at 373 and 573 K (spectra 8 and 9, respectively).

acid sites (capable of protonating DMP) on the  $\gamma$ -Ga<sub>2</sub>O<sub>3</sub> surface. On the activated samples, it is difficult to specify which OH groups give rise to DMPH<sup>+</sup> species since, as in the case of pyridine, DMP coordination also affects several OH groups. However, the subtracted spectrum, 1 minus 4, in the  $\nu$ (OH) range (spectrum after DMP outgassing at 423 K minus that after outgassing at room temperature) shows that, in addition to the 3693 cm<sup>-1</sup> band sensitive to DMP coordination, the  $\nu$ (OH) band at about 3650 cm<sup>-1</sup> is also perturbed (Figure 3, spectrum 4). This suggests that some DMPH<sup>+</sup> species could result from the interaction of DMP with OH groups giving rise to the 3650 cm<sup>-1</sup> band.

DMPH<sup>+</sup> species disappear after outgassing at 423 K (Figure 3, spectrum 4). By contrast, bands at 1605, 1574, and 1455 cm<sup>-1</sup> persist even after outgassing at 673 K (Figure 3, spectrum 7). This would suggest that DMP species coordinated to Lewis acid sites have a relatively high thermal stability. However, the shift of their frequencies (they are situated at 1613, 1580, and 1465 cm<sup>-1</sup> after outgassing at room temperature and at 1605, 1574, and 1455 cm<sup>-1</sup> after outgassing at 673 K), the disappearance of the 1401 and 1383 cm<sup>-1</sup> bands upon outgassing at an increasing temperature, and the appearance of a new band at 1080 cm<sup>-1</sup> (not shown) indicate the onset of a thermal instability of adsorbed DMP.

Comparison with results obtained on alumina (Figure 3, spectra 8 and 9) shows that (i) the strength of Lewis acid sites is slightly higher on alumina (for instance, after outgassing at room temperature the  $\nu_{\text{sa}}$  band appears at 1617 cm<sup>-1</sup> on alumina instead of at 1613 cm<sup>-1</sup> on gallia) and (ii) the thermal stability of DMP-coordinated species is higher on alumina than on gallia, since on the former no relevant changes were seen even after outgassing at 573 K (spectra not shown).

**3.3. IR Spectra of Adsorbed CD<sub>3</sub>CN.** Acetonitrile is often used as a molecular probe for both acidic and basic centers on the surface of metal oxides. It interacts with Lewis and Brønsted acid sites through the electron lone pair located on the nitrogen atom, giving rise to a blue shift of the  $\nu$ (C≡N) band. The larger the shift, the more acidic the sites.<sup>28</sup> For CH<sub>3</sub>CN, the  $\nu$ (C≡N) vibration is split due to a Fermi resonance with the  $\nu$ (C–C) +  $\delta$ (CH<sub>3</sub>) combination mode, and this fact perturbs determination

of the  $\nu$ (C≡N) shift. Use of CD<sub>3</sub>CN is preferred since now the  $\nu$ (C≡N) vibration is not perturbed by Fermi resonance. This mode appears at 2265 cm<sup>-1</sup> in free CD<sub>3</sub>CN.

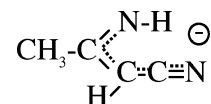
When acetonitrile interacts with basic sites (anions) at the surface of metal oxides, several species can be formed:<sup>29</sup>

(i) The CH<sub>2</sub>CN<sup>-</sup> species can be formed through the surface reaction



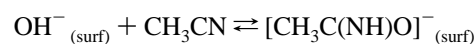
The  $\nu$ (C≡N) vibration of the CH<sub>2</sub>CN<sup>-</sup> species is expected to be in the 2000–2100 cm<sup>-1</sup> range.

(ii) When large amounts of acetonitrile are added, dimerization can occur leading to the anion dimer species. This dimer

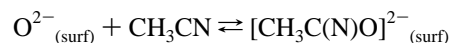


species is characterized by a  $\nu$ (NH) band near 3330 cm<sup>-1</sup> and a  $\nu$ (C≡N) band near 2120 cm<sup>-1</sup> (close to the  $\nu_s$ (CD<sub>3</sub>) vibration mode when CD<sub>3</sub>CN is used).

(iii) Acetamide species can also be formed, either the monoanion [CH<sub>3</sub>C(NH)O]<sup>-</sup>



or the dianion [CH<sub>3</sub>C(N)O]<sup>2-</sup>



They are both characterized by very strong IR absorption bands in the 1600–1500 cm<sup>-1</sup> range and also by bands near 1430–1440 and 1170 cm<sup>-1</sup>. These bands are all sensitive to the CH<sub>3</sub> ⇌ CD<sub>3</sub> substitution. The way to discriminate between the mono- and the dianion species is by determining the OH<sub>(surf)</sub> ⇌ OD<sub>(surf)</sub> effect on their frequency. As expected, only those IR absorption bands characteristic of the monoanion are sensitive to the isotopic effect. In particular, that near 1170 cm<sup>-1</sup> is displaced to about 960 cm<sup>-1</sup> after surface deuteration.

Spectra 1 and 2 in Figure 4 correspond to CD<sub>3</sub>CN adsorbed on  $\gamma$ -Ga<sub>2</sub>O<sub>3</sub> previously activated at 973 and 673 K, respectively. The 2310–2308 cm<sup>-1</sup> band is due to CD<sub>3</sub>CN coordinated to Lewis acid sites. The 2261–2259 cm<sup>-1</sup> sharp band, appearing when a large amount of CD<sub>3</sub>CN is added and disappearing by outgassing at room temperature, characterizes physisorbed CD<sub>3</sub>CN. The 2111 cm<sup>-1</sup> band is due to  $\nu_s$ (CD<sub>3</sub>) of coordinated or physisorbed CD<sub>3</sub>CN. A broad band near 2230 cm<sup>-1</sup>, which is more resistant to outgassing at a progressively higher temperature, could correspond to polymerization products. Below 1700 cm<sup>-1</sup>, there are five main bands at 1558, 1508, 1460, 1388, and 1305 cm<sup>-1</sup>. Also, a band near 1250 cm<sup>-1</sup> is observed. This latter band gains intensity after outgassing at a moderate temperature, 373 and 473 K (spectra 5 and 6). Comparison between spectra on  $\gamma$ -Ga<sub>2</sub>O<sub>3</sub> activated at 673 and 973 K (Figure 4, spectra 2 and 1, respectively) shows that they have the same bands, i.e., acetonitrile adsorption is qualitatively insensitive to the hydroxylation degree of the sample surface, which is in favor of dianion formation. Moreover, the spectrum recorded after CD<sub>3</sub>CN adsorption on  $\gamma$ -Ga<sub>2</sub>O<sub>3</sub> exchanged with D<sub>2</sub>O (spectrum 3) shows the same bands as before, confirming their insensitivity to the OH/OD exchange and hence the dianion character of the species formed.

According to this interpretation, it could be expected that hydroxy groups are not directly involved in acetonitrile adsorp-

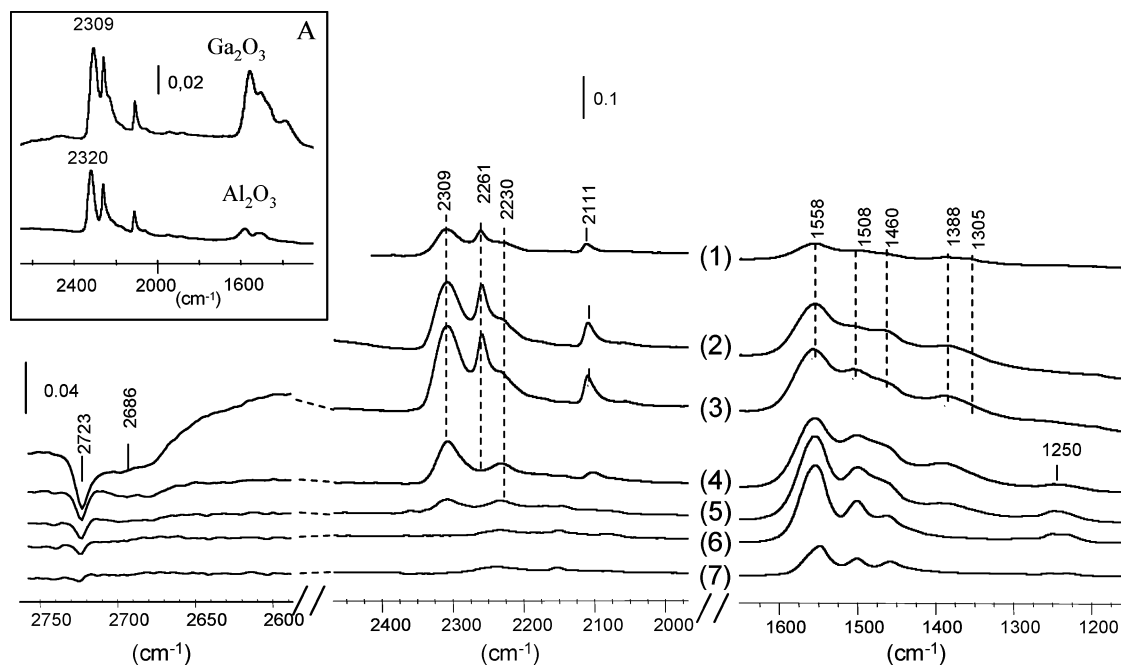


**Figure 4.** IR difference spectra of  $\text{CD}_3\text{CN}$  adsorbed at room temperature on  $\gamma\text{-Ga}_2\text{O}_3$  at an equilibrium pressure of 1 Torr. (1)  $\gamma\text{-Ga}_2\text{O}_3$  activated at 973 K; (2) activated at 673 K; (3)  $\text{CD}_3\text{CN}$  (1 Torr) adsorbed at room temperature on deuterated  $\gamma\text{-Ga}_2\text{O}_3$  activated at 673 K; (4–7) after outgassing for 30 min at room temperature at 373, 473, and 573 K, respectively. Inset A: Comparison between the IR spectra of  $\gamma\text{-Ga}_2\text{O}_3$  and  $\gamma\text{-Al}_2\text{O}_3$  activated at 673 K having 1 Torr of adsorbed  $\text{CD}_3\text{CN}$ .

tion. However, they are still perturbed. After  $\text{CD}_3\text{CN}$  adsorption and outgassing at room temperature on the deuterated  $\gamma\text{-Ga}_2\text{O}_3$  sample, difference spectra show that both hydroxy groups giving rise to  $\nu(\text{OD})$  bands at 2723 and 2686  $\text{cm}^{-1}$  are partly affected (Figure 4, spectrum 3). After outgassing at 473 K, the two  $\nu(\text{OD})$  bands are (nearly) restored (Figure 4, spectrum 6), and the  $\nu(\text{CN})$  band of the coordinated species at 2309  $\text{cm}^{-1}$  is no longer observed, whereas bands of acetamide species are still present. This suggests that perturbation of hydroxy groups by acetonitrile adsorption results from an indirect effect induced by coordination of  $\text{CD}_3\text{CN}$  species to neighboring Lewis acid sites, as already documented<sup>17,30</sup> for acetonitrile adsorbed on alumina. Comparison between results obtained for  $\text{CD}_3\text{CN}$  adsorbed on  $\gamma\text{-Ga}_2\text{O}_3$  and on  $\gamma\text{-Al}_2\text{O}_3$  activated at 673 K (Figure 4A, inset) clearly shows that acetamide species are much less abundant on alumina. As expected from the previous pyridine adsorption results, the  $\nu(\text{CN})$  vibration of coordinated  $\text{CD}_3\text{CN}$  species occurs at a higher wavenumber on alumina (2320  $\text{cm}^{-1}$ ) than on  $\gamma\text{-Ga}_2\text{O}_3$  (2309  $\text{cm}^{-1}$ ). However, such a comparison is now more complicated than that in the case of pyridine, due to the large amount of acetamide species simultaneously formed on  $\gamma\text{-Ga}_2\text{O}_3$ . It has been already reported that preadsorption of base probe molecules modifies the subsequent adsorption behavior of an acid site, as observed on alumina from coadsorption of  $\text{CO}_2$  and pyridine<sup>31</sup> and on zinc oxide for  $\text{CO}$  and  $\text{CO}_2$ .<sup>32</sup>

**3.4. IR Spectra of Adsorbed Carbon Dioxide.**  $\text{CO}_2$  was used to probe the basicity of both metal oxides. The IR spectra, in the 1900–1150  $\text{cm}^{-1}$  wavenumber range of carbon dioxide adsorbed at room temperature on  $\gamma\text{-Ga}_2\text{O}_3$  and  $\gamma\text{-Al}_2\text{O}_3$  are shown in Figure 5. On alumina (spectrum 2), two main species can be considered. One of them gives rise to bands in the 1750–1900 and 1150–1200  $\text{cm}^{-1}$  ranges. These bands can be assigned to either organic-like carbonate species or bent  $\text{CO}_2$ .<sup>33</sup> The second type of adsorbed species is characterized mainly by the sharp bands at 1648, 1485, and 1234  $\text{cm}^{-1}$ , which can be unambiguously assigned to hydrogen-carbonate species.<sup>18,34</sup> On gallia (spectrum 1), the latter species gives rise to bands at 1619,

1456, and 1231  $\text{cm}^{-1}$ , which are superimposed with a broader band centered at 1450  $\text{cm}^{-1}$  due to (ionic) carbonate species. The broadness of this carbonate band suggests some heterogeneity of the basic surface sites.

The spectra in Figure 5 have been normalized to 100  $\text{m}^2 \text{g}^{-1}$ . The main purpose of doing this is to show the high intensity of the  $\delta(\text{OH})$  band of hydrogen-carbonate species at 1231  $\text{cm}^{-1}$  for  $\gamma\text{-Ga}_2\text{O}_3$  as compared to the corresponding band (at 1234  $\text{cm}^{-1}$ ) for  $\gamma\text{-Al}_2\text{O}_3$ . A higher concentration of hydrogen-carbonate species on  $\gamma\text{-Ga}_2\text{O}_3$  (as compared to that on  $\gamma\text{-Al}_2\text{O}_3$ ) is also confirmed by the higher intensity of the  $\nu(\text{OH})$  band at 3607  $\text{cm}^{-1}$  on  $\gamma\text{-Ga}_2\text{O}_3$ , compared to the corresponding band at 3608  $\text{cm}^{-1}$  on  $\gamma\text{-Al}_2\text{O}_3$  (Figure 5B). Difference spectra in the 3800–3300  $\text{cm}^{-1}$  frequency range show that on gallia hydroxy groups at 3693  $\text{cm}^{-1}$  are mainly involved in the formation of hydrogen-carbonate species.

For both,  $\gamma\text{-Ga}_2\text{O}_3$  and  $\gamma\text{-Al}_2\text{O}_3$ , outgassing of  $\text{CO}_2$  at room temperature (Figure 5, spectra 3 and 4) leads essentially to a decrease of band intensity of organic-like carbonate species. When the outgassing was performed at 373 K (spectra not shown), desorption of most of the carbonate species, except for a small amount of hydrogen carbonates, was observed. Increasing the outgassing temperature up to 473 K led to complete desorption of all of the surface carbonate species, for both gallia and alumina. Such a behavior suggests that none of the metal oxides presents a strong basicity.

#### 4. Discussion

The main purpose of this study was to acquire information on the surface properties of  $\gamma\text{-Ga}_2\text{O}_3$ , a metal oxide for which no extended studies on its surface chemistry have been reported yet. Like gamma-alumina,  $\gamma$ -gallia presents a cubic spinel-type structure as confirmed by the X-ray diffraction pattern of the sample used.<sup>2,4</sup> Accordingly, the  $^{71}\text{Ga}$  magic angle spinning NMR spectrum<sup>4</sup> showed two main bands at about 70 and 200 ppm, which are characteristic of gallium in 6-fold ( $\text{Ga}_{\text{VI}}$ ) and 4-fold ( $\text{Ga}_{\text{IV}}$ ) coordination to oxygen, respectively. However

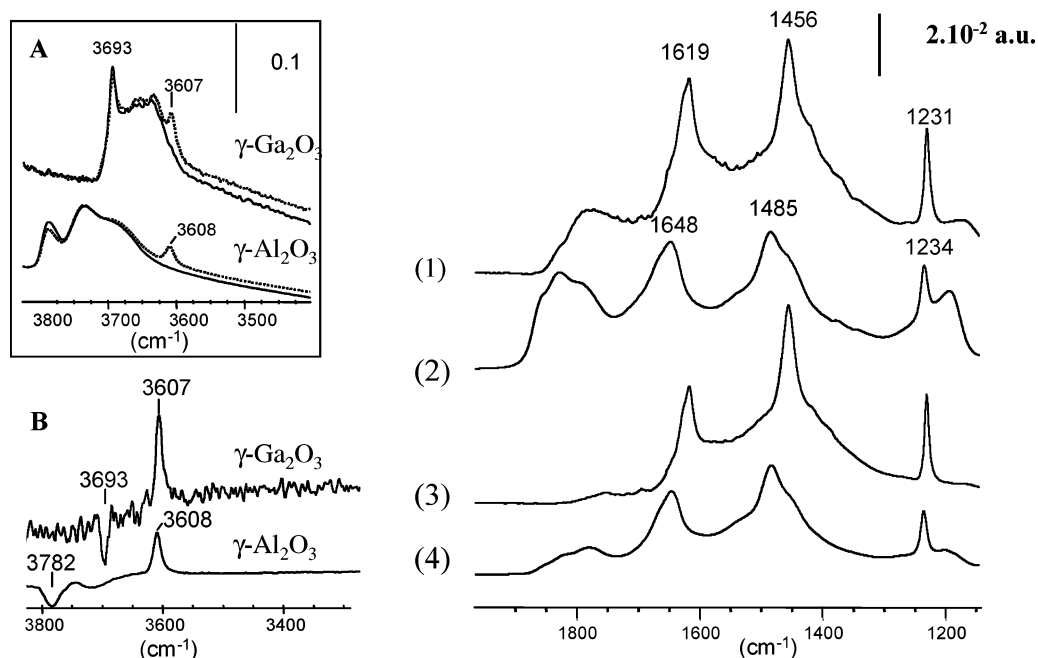


**Figure 5.** Room-temperature IR spectra of (1)  $\gamma$ -Ga<sub>2</sub>O<sub>3</sub> having 5 Torr (equilibrium pressure) of adsorbed CO<sub>2</sub>; (3) after outgassing for 30 min at room temperature; (2)  $\gamma$ -Al<sub>2</sub>O<sub>3</sub> having 5 Torr (equilibrium pressure) of adsorbed CO<sub>2</sub>; (4) after outgassing for 30 min at room temperature. The blank spectra of  $\gamma$ -Ga<sub>2</sub>O<sub>3</sub> and  $\gamma$ -Al<sub>2</sub>O<sub>3</sub> were subtracted from 1 and 3 and 2 and 4, respectively. Inset A:  $\nu$ (OH) bands of hydroxy groups of activated  $\gamma$ -Ga<sub>2</sub>O<sub>3</sub> before and after CO<sub>2</sub> adsorption. Inset B: OH stretching region of the IR difference spectra of CO<sub>2</sub> adsorbed on  $\gamma$ -Ga<sub>2</sub>O<sub>3</sub> and  $\gamma$ -Al<sub>2</sub>O<sub>3</sub> (blank spectrum subtracted, in both cases).

these techniques do not give relevant information on surface structure and properties. By contrast, IR spectroscopy enables surface properties to be characterized from both the study of residual hydroxy groups and analysis of IR spectra of adsorbed probe molecules.

**4.1. Hydroxy Groups.** When thermally activated, finely divided metal oxides present residual OH groups having IR stretching frequencies related to the nature of surface cations.<sup>35</sup> The present study shows that the stretching frequency of the free OH groups on the surface of  $\gamma$ -Ga<sub>2</sub>O<sub>3</sub> (3693 and about 3660 cm<sup>-1</sup>) is lower than that shown by  $\gamma$ -Al<sub>2</sub>O<sub>3</sub> (3780, 3730, 3680 cm<sup>-1</sup>). This fact can be related<sup>36</sup> to the greater ionic radius and consequently smaller charge-to-radius ratio of the Ga<sup>3+</sup> ion compared to Al<sup>3+</sup>.

For alumina, the multiplicity of the  $\nu$ (OH) bands has been explained by invoking (i) the multifold coordination of the hydroxyls themselves (linear species giving rise to  $\nu$ (OH) bands at a higher frequency than that characterizing bridged species), (ii) the coordination number of the cation to which OH groups are bound, and (iii) the presence of morphologic defects on the surface (edges, corners, etc.).<sup>37</sup> All of these features have been invoked to explain the multiplicity of OH groups on the surface of alumina. According to Tsyganenko and Filimonov<sup>38</sup> and to Knozinger and Ratnasamy,<sup>39</sup> three main types of OH groups should be considered depending on the number of cations bonded to the oxygen atom of the hydroxy group being considered. An additional subdivision may occur as a consequence of the coordination symmetry (tetrahedral or octahedral) of the cations involved. Moreover, the degree of crystallinity of the metal oxide can be related to a specific hydroxy group<sup>17</sup> characterized by a band at 3775 cm<sup>-1</sup>; well-crystallized alumina samples give rise to two high-frequency  $\nu$ (OH) bands at 3790 and 3775 cm<sup>-1</sup> whereas the spectra of amorphous samples usually present only a single broad band at about 3790 cm<sup>-1</sup>.

The  $\nu$ (OH) band at the higher wavenumber (3693 cm<sup>-1</sup>) in the spectrum of activated Ga<sub>2</sub>O<sub>3</sub> (Figure 1) should be assigned to linear hydroxy groups. It is difficult to conclude the

coordination number of the Ga<sup>3+</sup> cation involved, since literature reports on alumina are conflicting. Busca et al.<sup>36</sup> consider that the high-frequency  $\nu$ (OH) bands correspond to Al<sub>IV</sub>-OH groups whereas Knozinger and Ratnasamy<sup>39</sup> proposed Al<sub>VI</sub>-OH groups for the highest wavenumber band. The comparison among iron, magnesium, and aluminum spinels and also corundum-type metal oxide powders showed that OH groups bound to cations having a lower coordination number give rise to higher-frequency  $\nu$ (OH) bands.<sup>36</sup> A previous study<sup>4</sup> has shown that the intensity of the 3693 cm<sup>-1</sup> band is much lower on  $\alpha$ -Ga<sub>2</sub>O<sub>3</sub> than that on  $\gamma$ -Ga<sub>2</sub>O<sub>3</sub>, which would suggest that this band characterizes Ga<sub>IV</sub>-OH groups.

However, the sharpness of the 3693 cm<sup>-1</sup> band in the spectrum of  $\gamma$ -Ga<sub>2</sub>O<sub>3</sub> (Figure 1) is surprising for a rather amorphous material. Its full width at half-maximum is close to that reported for the 3745 cm<sup>-1</sup> silanol band on silica. It is known<sup>40</sup> that the presence of silica as a surface impurity on metal oxides can lead to a sharp band at a lower wavenumber than that observed for pure silica. Nevertheless, 3693 cm<sup>-1</sup> is a very low frequency for such an assignment. Moreover, in that case, a substantial Brønsted acidity should be expected,<sup>41</sup> whereas the number of Brønsted acid sites detected by DMP adsorption on  $\gamma$ -Ga<sub>2</sub>O<sub>3</sub> is quite low.

However, the spectrum of  $\gamma$ -Ga<sub>2</sub>O<sub>3</sub> in the  $\nu$ (OH) range presents a pattern similar to that reported for MgO,<sup>42,43</sup> i.e., a sharp band at a high wavenumber (3740 cm<sup>-1</sup> in the case of MgO) and a broader one in the 3450–3650 cm<sup>-1</sup> range. Moreover, the fact that the highest frequency OH groups of  $\gamma$ -Ga<sub>2</sub>O<sub>3</sub> do not participate in the dehydroxylation process up to 573 K bears resemblance with the behavior shown by MgO, since it has been reported<sup>42</sup> that the intensity of the high-wavenumber OH band in MgO is also a little sensitive to thermal treatments. This high-wavenumber IR band (of MgO) has been assigned to OH groups attached to highly unsaturated cation sites (occurring at edges and corners of small crystals), while the broad band at about 3600 cm<sup>-1</sup> was assigned to OH groups on extended faces.<sup>42,43</sup> By analogy, we propose that the sharp



band at 3693  $\text{cm}^{-1}$  on  $\gamma\text{-Ga}_2\text{O}_3$  corresponds to OH groups located at highly unsaturated sites (defect sites) that are a distance apart among themselves, while the broad band covering the 3600–3660  $\text{cm}^{-1}$  range corresponds to OH groups situated on regular (extended) faces and that are closer together. This would explain why the hydroxyls responsible for the broader band are more easily eliminated (nucleating water) during the thermal treatment giving rise to partial dehydroxylation; it would also explain the broadness of the low-wavenumber band compared to the sharpness of the OH band at 3693  $\text{cm}^{-1}$ .

Whatever the probe used, adsorbed molecules strongly affect the intensity of the band at 3693  $\text{cm}^{-1}$ . It is specifically affected when hydrogen–carbonate species are formed after  $\text{CO}_2$  adsorption (Figure 5), and a decrease of its intensity occurs when coordinated DMP, pyridine, or  $\text{CD}_3\text{CN}$  species are formed on the  $\gamma\text{-Ga}_2\text{O}_3$  surface. The present study also shows (Figure 5) that the 3780  $\text{cm}^{-1}$  band of the alumina sample used is also affected by adsorbed pyridine and  $\text{CO}_2$ . Such a sensitivity whatever the probe molecule used was also reported for the band at 3775  $\text{cm}^{-1}$  on well-crystallized alumina, which has been assigned to hydroxy groups in defect crystallographic sites,<sup>17,18</sup> and it was also proposed that the high sensitivity of these hydroxy groups to probe molecule adsorption is due to the presence of Lewis acid sites in the neighborhood.<sup>17</sup>

**4.2. Acid–Base Surface Properties.** The four IR probe molecules used in the present study give complementary results since pyridine mainly characterizes Lewis acidity, DMP is more sensitive to the presence of weak Brønsted acidity,  $\text{CO}_2$  adsorption mainly involves basic OH groups, and acetonitrile facilitates access to the  $\text{O}^{2-}$  basic sites through formation of acetamide-type species.

**Lewis Acidity.** Results obtained (Figures 2–4) from adsorption of pyridine, DMP ( $\nu_{8a}$  bands), and  $\text{CD}_3\text{CN}$  ( $\nu(\text{CN})$  band above 2300  $\text{cm}^{-1}$ ) clearly show the presence of strong Lewis acid sites on the surface of activated  $\gamma\text{-Ga}_2\text{O}_3$ . However, their acid strength is slightly lower than that observed for  $\gamma\text{-Al}_2\text{O}_3$ . These Lewis acid sites are related to *cus*  $\text{Ga}^{3+}$  ions in the tetrahedral position, already seen<sup>2</sup> by CO adsorption at 77 K. Studies on a series of metal oxides have shown<sup>28</sup> that the Lewis acid strength deduced from the blue shift of the  $\nu_{8a}$ ,  $\delta s(\text{NH}_3)$ , and  $\nu(\text{CN})$  bands of coordinated pyridine, ammonia, and acetonitrile (respectively) can be correlated to the polarizing power of the cation. Therefore, the lower Lewis acid strength of tetrahedral *cus*  $\text{Ga}^{3+}$  ions can be explained by their lower polarizing power compared to that of  $\text{Al}^{3+}$  cations. This lower polarizing power toward the adsorbed molecule can be explained in terms of (i) the smaller charge-to-radius ratio of the  $\text{Ga}^{3+}$  ion and (ii) the smaller ionicity of the tetrahedral Ga–O bond (as compared to the corresponding Al–O bond). This smaller ionicity stems from the  $d^{10}$  electronic configuration of the  $\text{Ga}^{3+}$  ion, which results in an enhanced polarizing power toward surrounding oxygen anions of the oxide framework and consequently lower (net) electric charge on the gallium(III) cation.

Spectra of pyridine adsorbed on  $\gamma\text{-Al}_2\text{O}_3$  usually show one broad  $\nu_{8a}$  band on amorphous samples<sup>17</sup> but two  $\nu_{8a}$  bands (at about 1612 and 1625  $\text{cm}^{-1}$ ) on well-crystallized samples, assigned to two different Lewis acid surface sites.<sup>18</sup> Therefore, the broadness of the  $\nu_{8a}$  band of coordinated pyridine in the spectra of  $\gamma\text{-Ga}_2\text{O}_3$  (Figure 2) can be explained in terms of the low crystallinity of the sample studied, which would give rise to two (nonresolved) types of tetrahedral *cus*  $\text{Ga}^{3+}$  sites.

The concentration of Lewis acid sites detected on  $\gamma\text{-Ga}_2\text{O}_3$  and  $\gamma\text{-Al}_2\text{O}_3$  by adsorbed DMP and pyridine was estimated from

**TABLE 1: Surface Density of Lewis Acid Sites on  $\gamma\text{-Al}_2\text{O}_3$  and  $\gamma\text{-Ga}_2\text{O}_3$**

adsorbate	estimated density of coordinated species (molecule per $\text{nm}^{-2}$ )	
	$\gamma\text{-Al}_2\text{O}_3$	$\gamma\text{-Ga}_2\text{O}_3$
DMP (rt) <sup>a</sup>	0.25	0.4
DMP (373 K)	0.11	0.23
pyridine (rt) <sup>a</sup>	1	1.5
pyridine (373 K)	0.6	1

<sup>a</sup> rt = room temperature.

the integrated area of the  $\nu_{8a}$  and  $\nu_{19b}$  bands, respectively, assuming molar absorption coefficient values<sup>44</sup> of 5.3 and 1.8  $\text{cm}^2 \mu\text{mol}^{-1}$  for  $\epsilon(\nu_{8a})$  and  $\epsilon(\nu_{19b})$ , respectively. The corresponding values are reported in Table 1. For pyridine adsorbed on alumina, the results shown in Table 1 are in agreement with those reported from pyridine adsorption measurements on  $\eta$ -alumina activated in similar experimental conditions.<sup>45</sup> However, for both metal oxides, the number of Lewis sites detected by DMP is much lower than that detected by pyridine, although DMP is more basic. However, it is known that DMP is a less sensitive probe for Lewis acidity due to the steric hindrance of the methyl groups on the nitrogen lone pair.<sup>46</sup> The main conclusion from the data in Table 1 is the higher density of Lewis acid sites detected by both probe molecules on  $\gamma\text{-Ga}_2\text{O}_3$  as compared to  $\gamma\text{-Al}_2\text{O}_3$ . Morterra et al.<sup>18,45</sup> have proposed that the main coordination sites of pyridine on transition aluminas involve  $\text{Al}_{\text{IV}}$  surface sites, which suggests a higher concentration of *cus*  $\text{Ga}_{\text{IV}}$  on the surface of gallia than on alumina. Two reasons can be given for this observed fact. First,  $\text{Ga}^{3+}$  is known<sup>47–49</sup> to have a higher tetrahedral preference than  $\text{Al}^{3+}$  in spinels, and hence a higher concentration of surface  $\text{Ga}_{\text{IV}}$  sites is expected. Second, for equal thermal activation conditions, the dehydroxylation degree of gallia and alumina could well be different, which would influence the relative surface density of Lewis acid sites.

**Brønsted Acidity.** DMP, because of its higher basicity, is more sensitive to Brønsted acidity than pyridine. No Brønsted acid sites were detected by pyridine adsorption on  $\gamma\text{-Ga}_2\text{O}_3$  (Figure 2) whereas, in the same conditions, protonated species characterized by the weak band at 1649  $\text{cm}^{-1}$  (Figure 3) are observed after DMP adsorption. However, the intensity of this band is quite low. From experimental measurements,<sup>50</sup> the molar absorption coefficient of the 1649  $\text{cm}^{-1}$  band of the lutidinium species has been estimated to be 4  $\text{cm}^2 \mu\text{mol}^{-1}$ . Hence, the concentration of Brønsted acid sites on activated  $\gamma\text{-Ga}_2\text{O}_3$  at 673 K turns out to be smaller than  $5 \times 10^{-2}$  sites  $\text{nm}^{-2}$ . On  $\gamma\text{-Al}_2\text{O}_3$ , the lutidinium band, detected at 1652  $\text{cm}^{-1}$ , is also very weak and has an intensity close to that of the corresponding band on gallia, when the relative surface area of both metal oxides is taken into account. This suggests that both metal oxides under study possess a small fraction of the Brønsted acid sites that are strong enough to protonate adsorbed DMP but not sufficiently strong to form pyridinium species. IR spectroscopy data can be used to estimate the strength of Brønsted acid sites from the wavenumber of the  $\nu(\text{NH})$  band of the protonated pyridine species,<sup>51</sup> and the same applies to DMP. However, in the present case, the corresponding IR absorption band is so weak that the method cannot be confidently applied. Another way to estimate the strength of Brønsted acid sites is the study of the thermal stability of the lutidinium species formed.<sup>52</sup> The disappearance of the corresponding bands after outgassing at 373 K (Figure 3) confirms the weak Brønsted acidic character of the hydroxy groups involved in the protonation of lutidine on both oxides. On  $\gamma\text{-Ga}_2\text{O}_3$ , these hydroxy groups could give

rise to the  $\nu(\text{OH})$  band at a low wavenumber (at about 3650  $\text{cm}^{-1}$ ). This would be in agreement with the general assumption that the lower the  $\nu(\text{OH})$  frequency and the higher the coordination number of the oxygen atom of the corresponding OH groups, the stronger their Brønsted acidity.

**Basicity.** The IR results obtained on both metal oxides show formation of hydrogen-carbonate species when CO<sub>2</sub> is adsorbed. Formation of these species was explained<sup>53–55</sup> by a nucleophilic attack of the oxygen atom of an OH group to the carbon atom of a coordinated CO<sub>2</sub> species on a neighboring site. According to such a mechanism, the surface sites revealed by CO<sub>2</sub> would be formed by a Lewis acid species and a nearby OH group. Our results (Figure 5) show that such pairs are slightly more abundant on  $\gamma$ -Ga<sub>2</sub>O<sub>3</sub> than on  $\gamma$ -Al<sub>2</sub>O<sub>3</sub> and that the OH groups involved would be characterized by the higher-wavenumber  $\nu(\text{OH})$  band.

Morterra et al.<sup>56</sup> reported that CO<sub>2</sub> adsorbed on alumina gives rise to formation of two types of hydrogen-carbonate species denoted as B1 and B2. The first one is observed only on partially dehydrated samples. The second one is predominant on samples outgassed above 573 K and involves  $\text{cus Al}_{\text{IV}}$  as the adsorption site. Consequently, the higher intensity of the hydrogen-carbonate bands on  $\gamma$ -Ga<sub>2</sub>O<sub>3</sub> results from the formation of a larger amount of B2 species, which would be related to the higher surface density of  $\text{cus Ga}_{\text{IV}}$  as discussed above.

IR spectra (Figure 5) indicate that other surface species, probably carbonates, are also formed by CO<sub>2</sub> adsorbed on both alumina and gallia. However, their detection is not straightforward since they give rise to bands superimposed with those characterizing hydrogen-carbonate species in the 1200–1700  $\text{cm}^{-1}$  wavenumber range. Bands at about 1750–1900 and 1150–1200  $\text{cm}^{-1}$  are more evident, but their assignment is not clear.<sup>57</sup> This is one reason complementary experiments on CD<sub>3</sub>-CN adsorption were performed.

IR spectra resulting from (deuterated or not) acetonitrile adsorbed on  $\gamma$ -Ga<sub>2</sub>O<sub>3</sub> (Figure 4) show that, in addition to coordinated species, acetamide species having a dianion character are also formed. These acetamide species are present in a larger amount on gallia than on alumina, thus showing that  $\gamma$ -Ga<sub>2</sub>O<sub>3</sub> presents on its surface a higher concentration of basic O<sup>2-</sup> sites. On alumina, Knozinger et al.<sup>58</sup> assumed that the acetamide monoanion is formed by a concerted mechanism involving acid-base pair sites consisting of  $\text{cus Al}^{3+}$  ions and basic OH groups. We propose that formation of the acetamide dianion on  $\gamma$ -Ga<sub>2</sub>O<sub>3</sub> also involves acid-base pair sites, the base center being a surface O<sup>2-</sup> anion.

**4.3. Redox Character.** It was reported that Ga<sub>2</sub>O<sub>3</sub> can be partially reduced by thermal treatment at 773 K under hydrogen<sup>59</sup> or by prolonged heating at 973 K under a vacuum.<sup>60</sup> And it is also known<sup>61,62</sup> that adsorption of IR probe molecules such as CO or CH<sub>3</sub>OH can lead to differentiation of Ce<sup>3+</sup> and Ce<sup>4+</sup> ions on ceria, an easily reducible metal oxide. However, IR spectra of several probe molecules (CH<sub>3</sub>OH, CO, pyridine, CD<sub>3</sub>-CN) on  $\gamma$ -Ga<sub>2</sub>O<sub>3</sub> previously treated under H<sub>2</sub> (not shown) did not produce any significant difference when compared with spectra obtained on the oxidized sample, and no direct spectroscopic evidence of the reduction of Ga<sup>3+</sup> ions on the surface of  $\gamma$ -Ga<sub>2</sub>O<sub>3</sub> was obtained in the present study. However, thermal desorption measurements of adsorbed pyridine and DMP (Figures 2 and 3) showed that chemical transformation of these adsorbed molecules occurs on  $\gamma$ -Ga<sub>2</sub>O<sub>3</sub> at a significantly lower temperature than on  $\gamma$ -Al<sub>2</sub>O<sub>3</sub>, thus suggesting a slight redox character of  $\gamma$ -gallia under the measurement conditions. In the same sense, work in progress on NO dissociation on hydrogen-

pretreated  $\gamma$ -Ga<sub>2</sub>O<sub>3</sub> samples seems to confirm that this metal oxide can have some redox activity.

## 5. Conclusions

While the surface chemistry of  $\gamma$ -Al<sub>2</sub>O<sub>3</sub> has been the subject of many experimental studies for several decades, much less is known about surface properties of the structurally related  $\gamma$ -Ga<sub>2</sub>O<sub>3</sub> oxide. Since gallium oxides are known to have relevant catalytic properties, it seemed desirable to study in some detail the surface chemistry of  $\gamma$ -Ga<sub>2</sub>O<sub>3</sub> and to compare it with that of  $\gamma$ -Al<sub>2</sub>O<sub>3</sub>. To this end we have (i) analyzed the OH IR spectra of  $\gamma$ -Ga<sub>2</sub>O<sub>3</sub> samples having a variable degree of surface hydroxylation, (ii) studied surface acidity and basicity of  $\gamma$ -Ga<sub>2</sub>O<sub>3</sub> by IR spectroscopy of adsorbed probe molecules (pyridine, DMP, CD<sub>3</sub>CN, and carbon dioxide), and (iii) compared the results obtained with those derived from parallel studies on a  $\gamma$ -Al<sub>2</sub>O<sub>3</sub> sample. The main conclusions obtained can be summarized as follows.

(i) Besides the expected small variation in the wavenumbers of characteristic O–H stretching bands, the OH spectrum of (hydroxylated)  $\gamma$ -Ga<sub>2</sub>O<sub>3</sub> shows a sharp (high-frequency) band at 3693  $\text{cm}^{-1}$  that is very resistant to thermal treatment under vacuum and does not seem to have a close analogue in the IR spectra of  $\gamma$ -Al<sub>2</sub>O<sub>3</sub>. This 3693  $\text{cm}^{-1}$  band of  $\gamma$ -Ga<sub>2</sub>O<sub>3</sub> was tentatively assigned to hydroxyl groups attached to coordinatively unsaturated tetrahedral Ga<sup>3+</sup> ions located at singular surface sites (e.g., corners of small crystals). A higher proportion of tetrahedrally coordinated cations in  $\gamma$ -Ga<sub>2</sub>O<sub>3</sub> than in  $\gamma$ -Al<sub>2</sub>O<sub>3</sub> (because of the higher tetrahedral preference of Ga<sup>3+</sup> as compared to Al<sup>3+</sup>) could be one reason for the observed difference between the corresponding OH IR spectra of these two metal oxides. However, it should also be pointed out that even for  $\gamma$ -Al<sub>2</sub>O<sub>3</sub> the OH bands appearing at the highest wavenumber (3790–3770  $\text{cm}^{-1}$ ) could also be related to singular (defective) surface sites rather than to hydroxyl groups located on regular sites as recently suggested by Digne et al.<sup>63</sup> from arguments based on density functional theory calculations.

(ii) Similar to what is known for  $\gamma$ -Al<sub>2</sub>O<sub>3</sub>, the Brønsted acidity of (partially hydroxylated)  $\gamma$ -Ga<sub>2</sub>O<sub>3</sub> was found to be very low, albeit not negligible. DMP adsorbed on  $\gamma$ -Ga<sub>2</sub>O<sub>3</sub> and  $\gamma$ -Al<sub>2</sub>O<sub>3</sub> shows, in both cases, a weak IR absorption band at 1649–1652  $\text{cm}^{-1}$  that identifies the protonated DMPH<sup>+</sup> species. However, no traces of the pyridinium ion were found when pyridine was adsorbed on either  $\gamma$ -Ga<sub>2</sub>O<sub>3</sub> or  $\gamma$ -Al<sub>2</sub>O<sub>3</sub>.

(iii) The surface Lewis acid strength was found to be slightly smaller in  $\gamma$ -Ga<sub>2</sub>O<sub>3</sub> than in  $\gamma$ -Al<sub>2</sub>O<sub>3</sub>. Since Lewis acidity is related mainly to tetrahedrally coordinated M<sup>3+</sup> ions (M = Al, Ga), the explanation for the above finding should rest on the smaller polarizing power of coordinatively unsaturated Ga<sub>IV</sub> ions, which have a smaller charge/radius ratio than Al<sup>3+</sup>. By contrast, the concentration of Lewis acid sites (detected by adsorbed pyridine and DMP) was found to be higher in  $\gamma$ -Ga<sub>2</sub>O<sub>3</sub> than in  $\gamma$ -Al<sub>2</sub>O<sub>3</sub>. This finding is most likely related to the higher tetrahedral preference of the Ga<sup>3+</sup> ion, as already pointed out.

(iv) Both  $\gamma$ -Ga<sub>2</sub>O<sub>3</sub> and  $\gamma$ -Al<sub>2</sub>O<sub>3</sub> showed a similar surface basicity toward adsorbed carbon dioxide and acetonitrile. However, the surface concentration of basic O<sup>2-</sup> ions was found to be larger for gallium oxide, as deduced from the larger amount of acetamide species formed upon adsorption of acetonitrile.

(v) Adsorbed pyridine and DMP were both found to be thermally more stable on  $\gamma$ -Al<sub>2</sub>O<sub>3</sub> than on  $\gamma$ -Ga<sub>2</sub>O<sub>3</sub>. The reason for this differential behavior is not known with certainty, but it



could well be associated with the slight redox character of gallium oxides.<sup>59,60</sup>

## References and Notes

- (1) Parenago, O. O.; Pushkar, Yu. N.; Turakulova, A. O.; Muraveva, G. P.; Lunina, E. V. *Kinet. Catal.* **1998**, *39*, 268.
- (2) Areán, C. O.; Bellan, A. L.; Mentrui, M. P.; Delgado, M. R.; Palomino, G. T. *Microporous Mesoporous Mater.* **2000**, *40*, 35.
- (3) Delgado, M. R.; Morterra, C.; Cerrato, G.; Magnacca, G.; Areán, C. O. *Langmuir* **2002**, *18*, 10255.
- (4) Lavalley, J. C.; Daturi, M.; Montouillout, V.; Clet, G.; Areán, C. O.; Delgado, M. R.; Sahibed-Dine, A. *Phys. Chem. Chem. Phys.* **2003**, *5*, 1301.
- (5) Thomas, J. M.; Liu, X. S. *J. Phys. Chem.* **1986**, *90*, 4843.
- (6) Inui, T.; Matsuda, H.; Yamase, O.; Nagata, H.; Fukuda, K.; Ukawa, T.; Miyamoto, A. *J. Catal.* **1986**, *98*, 491.
- (7) Kitagawa, H.; Sendoda, Y.; Ono, Y. *J. Catal.* **1986**, *101*, 12.
- (8) Khodakov, A. Yu.; Kustov, L. M.; Bondarenko, T. N.; Dergachev, A. A.; Kazansky, B. V.; Minachev, Kh. M.; Borbély, G.; Beyer, H. K. *Zeolites* **1990**, *10*, 603.
- (9) Nakagawa, K.; Kajita, C.; Ide, Y.; Okamura, M.; Kato, S.; Kasuya, H.; Ikenaga, N.; Kobayashi, T.; Suzuki, T. *Catal. Lett.* **2000**, *64*, 215.
- (10) Valey, P. *Chem. Eng.* **1991**, *491*, 13.
- (11) Li, Y.; Armor, J. N. *J. Catal.* **1994**, *145*, 1.
- (12) Freeman, D.; Wells, R. P. K.; Hutchings, G. J. *Chem. Commun.* **2001**, 1754.
- (13) Choudhary, V. R.; Jana, S. K.; Kiran, B. P. *J. Catal.* **2000**, *192*, 257.
- (14) Shimizu, K.; Satsuma, A.; Hattori, T. *Appl. Catal., B* **1998**, *16*, 319.
- (15) Shimizu, K.; Takamatsu, M.; Nishi, K.; Yoshida, H.; Satsuma, A.; Tanaka, T.; Yoshida, S.; Hattori, T. *J. Phys. Chem. B* **1999**, *103*, 1542.
- (16) Haneda, M.; Kintaichi, Y.; Hamada, H. *Appl. Catal., B* **1999**, *20*, 289.
- (17) Nortier, P.; Fourre, P.; Saad, A. B. M.; Saur, O.; Lavalley, J.-C. *Appl. Catal.* **1990**, *61*, 141.
- (18) Morterra, C.; Magnacca, G. *Catal. Today* **1996**, *27*, 497.
- (19) Boehm, H. P.; Knozinger, H. Nature and Estimation of Functional Groups on Solid Surfaces. In *Catalysis Science and Technology*; Anderson, J. R., Boudart, M., Eds.; Springer-Verlag: Berlin, 1984; Vol. 4.
- (20) Burneau, A.; Gallas, J.-P. In *The Surface Properties of Silicas*; Legrand, A. P., Ed.; John Wiley & Sons: 1998; Chapter 3A.
- (21) Davydov, A. A. In *Molecular Spectroscopy of Oxide Catalyst Surfaces*; Sheppard, N. T., Ed.; John Wiley & Sons: Hoboken, NJ, 2003.
- (22) Peri, J. B. *J. Phys. Chem.* **1965**, *69*, 211.
- (23) Wilson, E. B. *Phys. Rev.* **1934**, *45*, 706.
- (24) Delgado, M. R.; Areán, C. O. *Mater. Lett.* **2003**, *57*, 2292.
- (25) Morterra, C.; Chiorino, A.; Ghiotti, G.; Garrone, E. *J. Chem. Soc., Faraday Trans. 1* **1979**, *75*, 271.
- (26) Benesi, H. A. *J. Catal.* **1973**, *28*, 176.
- (27) Jacobs, P. A.; Heylen, C. F. *J. Catal.* **1974**, *34*, 267.
- (28) Busca, G. *Phys. Chem. Chem. Phys.* **1999**, *1*, 723.
- (29) Binet, C.; Jadi, A.; Lavalley, J.-C. *J. Chim. Phys. Phys.-Chim. Biol.* **1992**, *89*, 31.
- (30) Lavalley, J.-C.; Benaissa, M. *J. Chem. Soc., Chem. Commun.* **1984**, 908.
- (31) Morterra, C.; Chiorino, A.; Ghiotti, G.; Garrone, E. *J. Chem. Soc., Faraday Trans. 1* **1979**, *75*, 289.
- (32) Lavalley, J.-C.; Saussey, J.; Bovet, C. *J. Mol. Struct.* **1982**, *80*, 191.
- (33) Ramis, G.; Busca, G.; Lorenzelli, V. *Mater. Chem. Phys.* **1991**, *29*, 425.
- (34) Morterra, C.; Zecchina, A.; Coluccia, S.; Chiorino, A. *J. Chem. Soc., Faraday Trans. 1* **1977**, *73*, 1544.
- (35) Tsyganenko, A. A.; Mardilovich, P. P. *J. Chem. Soc., Faraday Trans.* **1996**, *92*, 4843.
- (36) Busca, G.; Lorenzelli, V.; Ramis, G.; Willey, R. J. *Langmuir* **1993**, *9*, 1492.
- (37) Davydov, A. A. In *Molecular Spectroscopy of Oxide Catalyst Surfaces*; Sheppard, N. T., Ed.; John Wiley & Sons: Hoboken, NJ, 2003, pp 56–59.
- (38) Tsyganenko, A. A.; Filimonov, V. N. *J. Mol. Struct.* **1973**, *19*, 579.
- (39) Knozinger, H.; Ratnasamy, C. *Catal. Rev.-Sci. Eng.* **1978**, *17*, 31.
- (40) Busca, G.; Saussey, H.; Saur, O.; Lavalley, J.-C.; Lorenzelli, V. *Appl. Catal.* **1985**, *14*, 245.
- (41) Areán, C. O.; Delgado, M. R.; Montouillout, V.; Lavalley, J.-C.; Fernandez, C.; Pascual, J. J. C.; Parra, J. B. *Microporous Mesoporous Mater.* **2004**, *67*, 259.
- (42) Coluccia, S.; Lavagnino, S.; Marchese, L. *Mater. Chem. Phys.* **1988**, *18*, 445.
- (43) Coluccia, S.; Lavagnino, S.; Marchese, L. *J. Chem. Soc., Faraday Trans. 1* **1987**, *83*, 477.
- (44) Vimont, A.; Lavalley, J.-C.; Francke, L.; Demourgues, A.; Tressaud, A.; Daturi, M. *J. Phys. Chem. B* **2004**, *108*, 3246.
- (45) Morterra, C.; Chiorino, A.; Ghiotti, G.; Garrone, E. *J. Chem. Soc., Faraday Trans. 1* **1979**, *75*, 271.
- (46) Jacobs, P. A.; Heylen, C. F. *J. Catal.* **1974**, *34*, 267.
- (47) Galasso, F. S. *Structure and Properties of Inorganic Solids*; Pergamon Press: New York, 1970.
- (48) Stone, F. S.; Areán, C. O.; Viñuela, J. S. D.; Platero, E. E. *J. Chem. Soc., Faraday Trans. 1* **1985**, *81*, 1255.
- (49) Areán, C. O.; Blanco, J. L. R.; Fernández, M. C. T. *J. Chem. Soc., Faraday Trans.* **1992**, *88*, 321.
- (50) Gaillard, M.; Mauge, F. Private communication.
- (51) Lavalley, J.-C.; Anquetil, R.; Czynievska, J.; Ziolk, M. *J. Chem. Soc., Faraday Trans.* **1996**, *92*, 1263.
- (52) Jacobs, P. A.; Heylen, C. F. *J. Catal.* **1974**, *34*, 267.
- (53) Busca, G.; Lorenzelli, V. *Mater. Chem.* **1982**, *7*, 89.
- (54) Tsyganenko, A. A.; Trusov, E. A. *Russ. J. Phys. Chem.* **1985**, *59*, 2602.
- (55) Lavalley, J. C. *Catal. Today* **1996**, *27*, 377.
- (56) Morterra, C.; Zecchina, A.; Coluccia, S.; Chiorino, A. *J. Chem. Soc., Faraday Trans. 1* **1977**, *73*, 1544.
- (57) Ramis, G.; Busca, G.; Lorenzelli, V. *Mater. Chem. Phys.* **1991**, *29*, 425.
- (58) Knozinger, H.; Krietenbrink, H.; Müller, H.-D.; Schulz, W. *Proc. Inter. Congr. Catal.*, 6th, 1976 **1977**, 183.
- (59) Meriaudeau, P.; Primet, M. *J. Mol. Catal.* **1990**, *61*, 227.
- (60) Areán, C. O.; Bonelli, B.; Palomino, G. T.; Safont, A. M. C.; Garrone, E. *Phys. Chem. Chem. Phys.* **2001**, *3*, 1223.
- (61) Binet, C.; Daturi, M. *Catal. Today* **2001**, *70*, 155.
- (62) Hickey, N.; Fornasiero, P.; Kaspar, J.; Gatica, J. M.; Bernal, S. *J. Catal.* **2001**, *200*, 181.
- (63) Digne, M.; Sautet, P.; Raybaud, P.; Euzen, P.; Toulhoat, H. *J. Catal.* **2002**, *211*, 1.